On the linewidth enhancement factor α in semiconductor injection lasers

K. Vahala, L. C. Chiu, S. Margalit, and A. Yariv
California Institute of Technology 128-95, Pasadena, California 91125

(Received 3 December 1982; accepted for publication 18 January 1983)

A simple model for the linewidth enhancement factor α and its frequency dependence in semiconductor lasers is presented. Calculations based on this model are in reasonable agreement with experimental results.

PACS numbers: 42.55.Bi, 42.55.Px, 72.70. + m

The subject of the linewidth enhancement factor α has been of key interest in the study of modal instability in gain guided semiconductor lasers and more recently, in characterizing the noise properties of semiconductor lasers.[1-3] Current interest in this quantity has centered on its role in the expression for the linewidth of a fundamentally broadened semiconductor laser.[2,3]

$$\Delta\nu = \Delta\nu_{ST}(1+\alpha^2), \tag{1}$$

where $\Delta\nu_{ST}$ is the linewidth predicted by the modified Schawlow Townes formula.[4] α is defined in terms of the real and imaginary parts of the complex susceptibility $\chi(n)$[2,3]:

$$\alpha = -\frac{d\chi_R(n)/dn}{d\chi_I(n)/dn}, \tag{2}$$

$$\chi(n) \equiv \chi_R(n) + \iota\chi_I(n), \tag{3}$$

where n is the carrier density. α contains an interband component and a free-carrier component. The interband component is normally dominant[5] and is the component considered in this letter. The value of α can be inferred from measurements of gain spectra combined with a subsequent Kramers–Kronig analysis[5] or from field spectrum linewidth versus power measurements.[6] Recently, its value was measured directly by modulating a semiconductor laser.[7] Although calculations of both gain and index spectra have been presented,[8,9] similar calculations of the spectral dependence of α are not available. The purpose of this letter is twofold: first, by way of a simple model to consider the material characteristics which determine the size of α, and second, to use this model to calculate α in the case of a semiconductor with parabolic bands. To achieve the former requires a departure from the standard Kramers–Kronig approach to calculate index spectra. Instead, we will calculate the complex susceptibility directly and apply Eq. (2).

Assuming rigorous k selection rules, states in the conduction band can couple (via stimulated or spontaneous transitions) only to states with the same crystal momentum in the valence band. Within each band states couple by electron-electron and electron-phonon scattering processes, and it is well known that the resulting intraband thermalization occurs on a time scale which is many orders of magnitude shorter than the interband thermalization. For time scales larger than the intraband thermalization time (typically < 1 ps) we will assume intraband states can be considered independent. Essentially, this reduces the conduction-valence band system to an ensemble of collisionally broadened two level systems with different transition energies. Considering one particular system, it is well known that the real and imaginary parts of its complex susceptibility are given by[10]

$$\hat{\chi}_R = A\,[P_c(n,\omega) - P_v(n,\omega)]\,\frac{\omega_L - \omega}{(\omega_L-\omega)^2 + 1/T_2^2}, \tag{4}$$

$$\hat{\chi}_I = A\,[P_c(n,\omega) - P_v(n,\omega)]\,\frac{1/T_2}{(\omega_L-\omega)^2 + 1/T_2^2}, \tag{5}$$

where ω is the transition linecenter frequency, ω_L the lasing frequency, T_2 the collisional broadening time (in this case the intraband collision time due to phase destroying collisions), n the carrier density, $P_c(n,\omega)[P_v(n,\omega)]$ the conduction (valence) band occupation probability (quasi-Fermi function) for electrons, and A is proportional to the dipole matrix element. Expressions of this form are valid provided $P_c(n,\omega)$ and $P_v(n,\omega)$ do not vary significantly over the time T_2 (i.e., rate equation approximation[10]). In a single mode semiconductor laser this condition is always satisfied. $\hat{\chi}_R$ and $\hat{\chi}_I$ have the familiar shapes illustrated in Fig. 1. The total susceptibility is the sum of $\hat{\chi}_R$ and $\hat{\chi}_I$ over all states.

$$\chi_R = \int_{-\infty}^{\infty} \rho(\omega)A\,[P_c(n,\omega) - P_v(n,\omega)] \times \frac{\omega_L - \omega}{(\omega_L-\omega)^2 + 1/T_2^2}\,d\omega, \tag{6}$$

$$\chi_I = \int_{-\infty}^{\infty} \rho(\omega)A\,[P_c(n,\omega) - P_v(n,\omega)] \times \frac{1/T_2}{(\omega_L-\omega)^2 + 1/T_2^2}\,d\omega, \tag{7}$$

where $\rho(\omega)$ is the effective density of states.

Nearly all calculations of the gain spectrum to date assume $T_2 = \infty$. This assumption causes the Lorentzian in Eq. (7) to collapse to a delta function so that

$$\chi_I|_{T_2=\infty} = A\pi\rho(\omega_L)[\,P_c(n,\omega_L) - P_v(n,\omega_L)]. \tag{8}$$

This function is proportional to the gain spectrum normally calculated under the assumption of rigorous k selection. In this analysis it weights $\hat{\chi}_R$ and $\hat{\chi}_I$ in the integrals for χ_R and χ_I. For this reason we call this function the gain envelope and illustrate it in Fig. 1 for the case of parabolic bands. It is interesting to note that when $T_2 = \infty$ Eq. (6) merely expresses the fact that χ_R is the Kramers–Kronig transform of χ_I.

Since $P_c(n,\omega)$ and $P_v(n,\omega)$ are determined by the Fermi distribution functions for the conduction and valence bands, they are functions of the carrier density or equivalently the quasi-Fermi levels. Assuming the former and applying Eq. (2) yields

 0003-6951/83/080631-03$01.00

$$\alpha(\omega_L) = -\int_{-\infty}^{\infty} \rho(\omega)[\,P_c'(n,\omega) - P_v'(n,\omega)]\,\frac{\omega_L - \omega}{(\omega_L - \omega)^2 + 1/T_2^2}\,d\omega \Big/ \int_{-\infty}^{\infty} \rho(\omega)[\,P_c'(n,\omega) - P_v'(n,\omega)]\,\frac{1/T_2^2}{(\omega_L - \omega)^2 + 1/T_2^2}\,d\omega, \tag{9}$$

where a prime indicates differentiation with respect to carrier density and A has been assumed independent of ω (i.e., energy-independent matrix element). Each integral in Eq. (9) has $\hat{\chi}_R$ or $\hat{\chi}_I$ weighted by the derivative of the gain envelope with respect to carrier density (i.e., the differential gain envelope function). This weighting action is depicted in Fig. 1. This curve shows the differential gain envelope to be positive at all frequencies ω. Therefore all contributions to the differential gain [denominator in Eq. (9)] will be positive. Contributions to the differential index [numerator in Eq. (9)], however, will be negative for transitions above $\omega_L (\omega > \omega_L)$ and positive for transitions below ω_L. Therefore, asymmetry of the differential gain envelope about the lasing frequency ω_L is reflected in the sign and size of α. It is, in fact, this asymmetry which causes α to be nonzero in semiconductor laser systems (or any other laser system exhibiting such an asymmetry). Since the differential gain envelope is larger above those frequencies with positive gain, α will be positive for lasing modes.

To illustrate the spectral behavior of α for several excitations we have calculated it using Eq. (9). The parabolic band effective density of states with effective masses characteristic of GaAs were used. T_2 was varied, but α remained relatively constant for 0.1 ps $< T_2 <$ 0.5 ps. $T_2 = 0.2$ ps was used for the plots shown in Fig. 2. Notice that α at a given frequency is larger for larger carrier densities. The shaded region corresponds to frequencies within one longitudinal mode spacing of the gain peak (assuming a 300-μm cavity length). Decrease of gain peak α under increased excitation is evident. This behavior has been observed by Henry *et al.*[5] Adding a free-carrier contribution of 0.8 (inferred from Ref. 5) to the interband α calculated here puts the total value of α in the range 3.2–4.2. This is compared to $\alpha = 4.5 \pm 1.0$ as measured by Harder, Vahala, and Yariv for an undoped active layer.[7] The insert to Fig. 2 illustrates the gain spectra corresponding to the various α spectra. These curves were calculated using Eq. (7) ("A" was assumed to be the Kane matrix element[11]). Transparency occurs for a carrier density of roughly 1.55×10^{18} cm^{-3}. This is slightly larger than calculated elsewhere[12] for parabolic bands with k selection, because this model accounts for smearing of the individual transitions due to intraband collisions. These collisions cause, according to Eq. (7), χ_I to be nonzero for photon energies $\hbar\omega_L < E_{\text{gap}}$ (i.e., in the energy gap) and thereby reduce the gain peak at a given carrier density as compared to calculations which assume $T_2 = \infty$.

In conclusion, we have presented a simple description of the linewidth broadening factor α and have also calculated the spectrum of α at various excitations for the simple

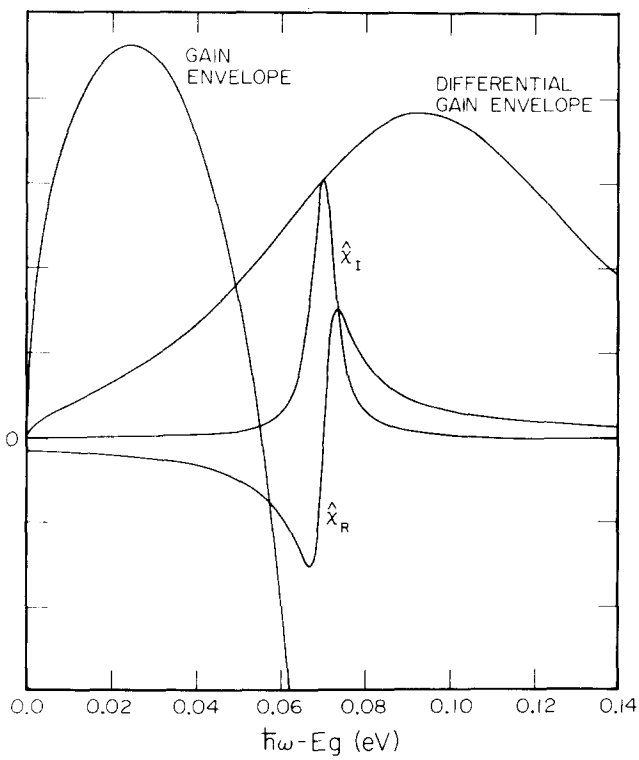

FIG. 1. Gain envelope function, and $\hat{\chi}_R$ and $\hat{\chi}_I$ weighted by the differential gain envelope function at an arbitrary frequency.

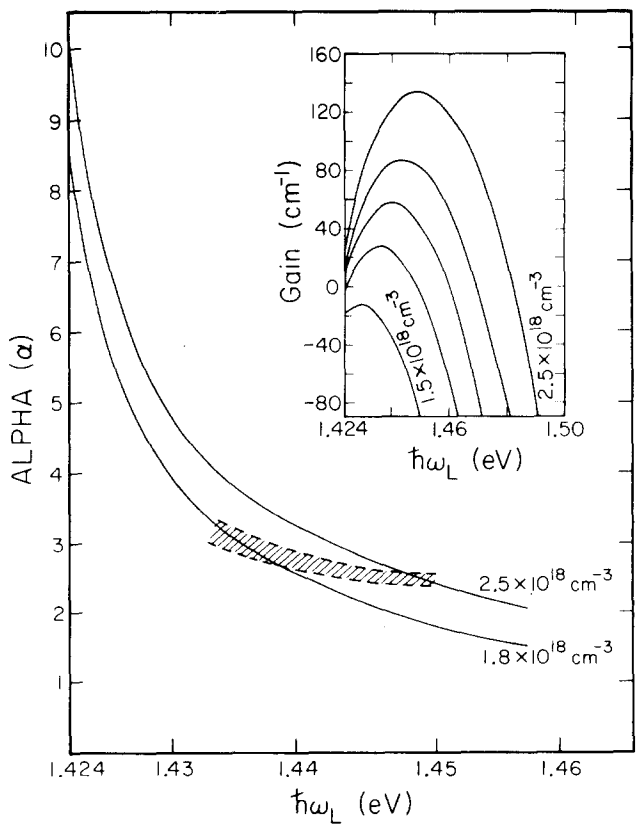

FIG. 2. α spectrum at several excitations. The shaded area corresponds to the region of peak gain. Insert: gain spectrum at several excitations.

case of parabolic bands. Results of this calculation are in reasonable agreement with direct measurements of α for an undoped active layer. The agreement may be fortuitous, however, since the actual situation is more complicated.

The authors acknowledge support from the National Science Foundation and Office of Naval Research. One author (K.J.V.) gratefully acknowledges support from the IBM corporation.

[1]R. Lang, IEEE J. Quantum Electron. **QE-15**, 718 (1979).
[2]C. H. Henry, IEEE J. Quantum Electron. **QE-18**, 259 (1982).
[3]K. Vahala and A. Yariv (to be published).
[4]A. Yariv, *Quantum Electronics* (Wiley, New York, 1975), p. 318.
[5]C. H. Henry, R. A. Logan, and K. A. Bertness, J. Appl. Phys. **52**, 4457 (1981).
[6]D. Welford and A. Mooradian, Appl. Phys. Lett. **40**, 865 (1982).
[7]Ch. Harder, K. Vahala, and A. Yariv, Appl. Phys. Lett. **42**, 328 (1983).
[8]G. H. B. Thompson, Opt. Electron. **4**, 257 (1972).
[9]F. Stern, J. Appl. Phys. **47**, 5382 (1976).
[10]M. Sargent III, M. Scully, and W. Lamb, *Laser Physics* (Addison-Wesley, Reading, Massachusetts, 1977), p. 104.
[11]H. C. Casey, Jr. and M. B. Panish, *Heterostructure Lasers, Part A* (Academic, New York, 1978), p. 146.
[12]C. H. Henry, R. A. Logan, and F. R. Merritt, J. Appl. Phys. **51**, 3042 (1980).

Index instabilities in proton-exchanged $LiNbO_3$ waveguides

Alfredo Yi-Yan
Centre National d'Etudes des Télécommunications, 196 rue de Paris, 92220 Bagneux, France

(Received 23 November 1982; accepted for publication 26 January 1983)

Measured effective mode indices on a day to day basis reveal an oscillatory behavior which indicates that the index profile of proton-exchanged $LiNbO_3$ waveguides evolves as a function of time. It is suggested that the profile instability might be brought about by a continuous migration of protons within the thickness of the guiding layer. Some index profile modificaiton may also be introduced during fabrication due to structural changes in the crystal as a function of exchange time.

PACS numbers: 42.80.Lt, 42.82. + n, 42.70.Fh, 84.40.Vt

In a recent communication, Jackel *et al.*[1] proposed a new technique to form optical waveguides in lithium niobate by the proton-lithium exchange process. The technique consists in immersing X-cut or Z-cut $LiNbO_3$ substrates into a molten bath of benzoic acid at some fixed temperature between 122 °C (melting point) and 249 °C (boiling point) for a given period of time which varies according to the required thickness for the guiding layer. The waveguides so obtained have been shown to have a steplike index profile with a maximum increase of 0.12 in the extraordinary index n_e at $\lambda = 633$ nm, the ordinary index n_0 being left unperturbed. Compared to the more established Ti:$LiNbO_3$ waveguides, proton-exchanged waveguides have the main advantages of their quick and economical method of fabrication and of their high Δn_e; the latter opens the possibility of realizing optical devices (e.g., sharp bends, lenses, etc...) for which the use of Ti:$LiNbO_3$ waveguides proved to be impractical.

This letter reports the existence of instabilities in the index profile of proton-exchanged $LiNbO_3$ waveguides. Measured effective mode indices on a day to day basis reveal an oscillatory behavior which indicates that the index profile evolves as a function of time. This "ageing" effect occurs under normal laboratory conditions and has not been found to disappear completely throughout an examination period of nearly two months.

Slab waveguides were formed using Z-cut, X-propagating, integrated optics grade (Crystal Technology) $LiNbO_3$ substrates which were immersed in an unstirred bath of benzoic acid at $T = 200 \pm 1$ °C using three different arrangements: (a) in an open stainless steel crucible, (b) in a closed quartz ampoule, and (c) in a vacuum-sealed quartz ampoule. While arrangement (a) allowed for substrate preheating before immersion into the bath, substrates for the other two arrangements were first loaded inside the ampoule with benzoic acid crystals at room temperature before being subjected to heating inside a furnace. By-products of the chemical attack of the acid on the Y facets of the substrates were best observed using the ampoule arrangements and immediately after removal from the furnace while the acid was still in the liquid phase. The experimental findings reported here apply, at least qualitatively, to all waveguides formed using all three arrangements. In what follows, only results obtained from waveguides formed using the closed ampoule arrangement will be presented.

Rutile prisms were used as input and output couplers to measure the effective mode indices N of the guided TM modes at $\lambda = 633$ nm. No guiding was observed for waves with the TE polarization. The experimentally measured dispersion diagram as a function of process time t_p (hours) is shown in Fig. 1 where the plotted values of N correspond to those measured shortly after removal of the samples from the furnace, followed by cleaning procedures with methanol. A qualitative inspection of the output m lines at this stage showed that their distribution followed closely that of true step-index waveguides.

Jackel and Rice[2] have recently shown that whereas par-

 0003-6951/83/080633-03$01.00